THE KINETICS OF REDUCTION OF NICKEL OXIDE–CERIUM DIOXIDE MIXED SYSTEMS WITH HYDROGEN AND THE EFFECT OF IONIZING RADIATION ON IT

Milan Pospíšil and Igor Petrecký

Department of Nuclear Chemistry,
Czech Technical University, 115 19 Prague 1

Received July 8th, 1983

The reduction with hydrogen is studied thermogravimetrically over the temperature region of 260—500°C for nickel oxide–cerium dioxide mixed systems of various composition. The overall rate of reduction increases and the maximum rate of reduction of nickel oxide decreases with increasing cerium dioxide content as a result of two counteracting processes occurring on the reaction interface and conditioned by the presence of the finely dispersed unreducible component. The dependence of the degree of reduction α on time t obeys the relation $(\alpha + 0{\cdot}3)/(1 - \alpha) = Ae^{kt}$ over the entire system composition region. Previous exposition of the samples to gamma doses of 100 and 500 kGy from a ^{60}Co source or to a fast neutron dose of 400 Gy from a ^{252}Cf source results in a decrease in the rate of reduction for region with excess nickel oxide, but as the concentration of cerium dioxide is increased, inversion of the radiation-induced effect takes place and the rate of reduction becomes higher than for the initial, unexposed samples. The effect of temperature and system composition on the phenomena under study is examined and discussed

Besides impregnation procedures, metal catalysts on oxide supports are frequently prepared by reduction of two-component mixed oxides where, for thermodynamic reasons, one of the components is not reduced or is reduced to lower oxidation states only. In the various composition regions the initial mixed oxides can form either homogeneous solid solutions[1,2] or separate phases[3]. In all cases the unreducible component affects the kinetics and degree of reduction[4] and also the activity of the final catalyst in dependence on the system composition, dispersity, preparation conditions, *etc.*[5,6].

In view of the ever-increasing importance of oxides of lanthanides as components in multicomponent catalysts[7] or supports[8], some physico-chemical properties of nickel oxide–cerium dioxide systems and the kinetics of their reduction with hydrogen are studied in this work over the entire region of their composition. The effect of previous exposition of the mixed oxides to gamma radiation or fast neutrons is also investigated.

EXPERIMENTAL

The mixed oxides of different composition were prepared by thermal decomposition of the mixed nitrates. Solutions of $Ce(NH_4)_2(NO_3)_6.6\,H_2O$ and $Ni(NO_3)_2.6\,H_2O$ of reagent grade purity

in a concentration of 1 mol l^{-1} were mixed in the desired proportions and evaporated to dryness, and the crystalline products were annealed in an electric resistance furnace in air at 200°C for 1 h and at 400°C for 3 h, and ground to powder in an agate mortar.

Nickel content in the samples was determined chelatometrically after separation with diacetyldioxime, cerium was determined iodometrically after oxidation with ammonium persulphate. The microstructure of the mixed oxides was examined by the Debye–Scherrer method on a TUR M 62 instrument (Carl Zeiss, Jena) equipped with a goniometer (Cu-anode). The size of the coherent regions of the two oxides was calculated from the broadening of the diffraction lines. The specific surface areas were obtained by the method of low-temperature adsorption of nitrogen. The morphology of the mixed oxides and the reduced samples was observed on a Jeol JSM-50 scanning electron microscope. Portions of the samples were exposed to 100 and 500 kGy doses of gamma radiation from a ^{60}Co source and to a dose of 400 Gy of fast neutrons of 2·1 MeV energy from a ^{252}Cf source (Radiochemical Centre, Amersham). The amount of the chemisorbed overstoichiometric oxygen (oxidation power of the surface) was determined iodometrically[9] for both the initial and the irradiated samples. The reduction was examined over the temperature region of 260—500°C under identical conditions for the initial and the irradiated mixed oxides. The kinetics of reduction was studied thermogravimetrically[10] in conditions where for all samples the time course and rate of the reduction were independent of the hydrogen flow rate. Sample portions of 50 mg were taken and the hydrogen flow rate was adjusted to 56 ml min^{-1}.

RESULTS AND DISCUSSION

Physico-Chemical Properties of the Mixed Oxides

The composition of the mixed oxides, their specific surface area, and the size of the coherent regions of the two components are given in Table I. The majority components of the system are nickel oxide and cerium dioxide forming separate phases. The size of the specific surface areas for both of them depends on the system composition in a nonmonotonic manner and generally correlates with the grain size. The electron microscope photographs at low magnifications (Fig. 1*) show that samples with nickel oxide predominating and with larger surface areas contain spherical aggregations 200—400 μm in size, in interaction with the finely dispersed cerium dioxide. The grain dispersity for both components is highest in samples No 9—11 (Table I) possessing the largest specific surface areas. Table I also shows that the size of microcrystallites of cerium dioxide is considerably smaller than that of nickel oxide and is virtually independent of the system composition. The mixed oxides with excess cerium dioxide therefore are more susceptible to heat treatment; as cerium dioxide concentration is increased, the surface area of samples subjected to heat treatment at 500°C for 1 h in air decreases monotonically to 87—36% of the initial value. Sample No 5, characterized by a very small surface area, displays a relatively stable surface structure which does not change on the heat treatment. For the remaining samples the sintering process during the heat treatment is associated with agglomeration of the microcrystallites and increase in the grain size, and the reduction process slows down.

* See insert on the p. 2240.

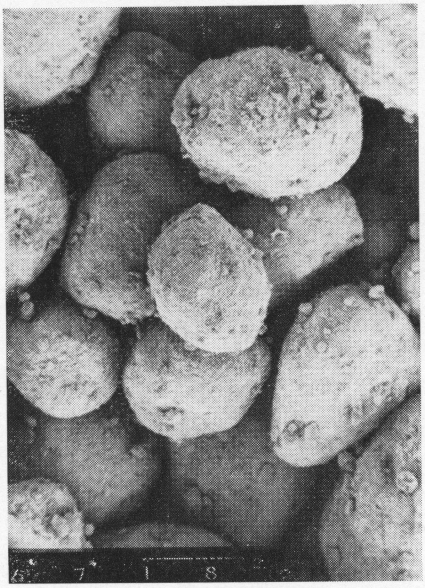

FIG. 1

Morphology of sample No 15. Magnification 100×; the line segment shown corresponds to 200 μm

The results of the iodometric determination of the amount of overstoichiometric oxygen, or the oxidation power of the surface, and this amount normalized with respect to the sample surface area are given in Table II. For the *p*-semiconductor nickel oxide this quantity corresponds to the surface concentration of Ni^{3+} ions which are in equilibrium with the ionogenic (chemisorbed) forms of oxygen. Provided that the *n*-semiconductivity of cerium dioxide is associated with the presence of interstitial Ce^{4+} ions[11], these surface ions, charge-compensated by chemisorbed oxygen, can also be detected iodometrically. The marked maximum of the normalized amount of chemisorbed oxygen in the region of high excess of cerium dioxide (sample No 5) and the similar lower maximum in the region of excess nickel oxide (95% (m/m) NiO) give evidence of a high extent of the mutual interaction between the two components in the two side composition regions. The oxidation power of the surface increasing with increasing concentration of the minority component up to a limiting value may be due to the increasing concentration of the catalytic centres constituted by ion pairs, requisite for the dissociative adsorption of oxygen molecules[12]. In addition to the pairs containing the ions of the two pure components (Ce^{3+}–Ce^{3+},

TABLE I

Composition of the NiO + CeO_2 samples, their specific surface area *S* and coherent regions size *L*

Sample No	Composition, % (m/m)			*S* $m^2\ g^{-1}$	*L*, nm	
	NiO	CeO_2	NiO + CeO_2		NiO	CeO_2
1	0·00	98·25	98·25	4·4	—	16·7
2	1·97	96·02	97·99	4·6	—	15·8
3	2·87	95·36	98·23	1·9	—	14·8
4	5·32	92·77	98·09	1·8	—	13·2
5	8·99	89·37	98·36	2·2	—	12·6
6	19·21	78·44	97·65	10·9	45·5	11·8
7	30·87	67·11	97·98	17·8	71·2	14·0
8	41·12	56·40	97·52	19·3	52·6	13·2
9	49·09	48·12	97·21	36·5	28·2	13·6
10	58·08	39·74	97·82	31·8	44·8	11·3
11	68·73	29·02	97·75	22·0	31·8	15·3
12	80·15	18·70	98·85	17·9	35·4	13·6
13	90·46	7·21	97·67	16·2	40·2	—
14	91·26	6·83	98·09	12·9	37·6	—
15	95·17	3·22	98·39	8·2	40·2	—
16	97·09	1·50	98·59	13·2	34·4	—
17	98·70	0·00	98·70	10·8	35·4	—

Ni^{2+}–Ni^{2+}), where for cerium dioxide the centres are composed of the lower-valency Ce^{3+} ions present in trace concentrations[11], the mixed pairs begin to play a role as the concentration of the minority component is increased, and these pairs are also oxidized to their higher valency states on the adsorption of oxygen:

$$Ce^{3+}\text{–}Ni^{2+} + O_2 \rightarrow Ce^{4+}\text{–}Ni^{3+} + 2O^- . \qquad (A)$$

If the concentration of the minority component is further increased, the nature of the mutual interaction of the two oxides changes so that the above centres, present in a smaller amount, cannot take part in the chemisorption, and the amount of oxygen decreases.

The effect of ionizing radiation on the amount of chemisorbed oxygen can be described by the parameter $\Delta X\,(\%) = 100(X^* - X)/X$, where X^* and X are the amounts of ionogenic oxygen present on the irradiated and nonirradiated samples, respectively. The dependence of ΔX on the composition of the mixed oxides is shown in Fig. 2. This parameter is positive for any composition. The trend of the dependence on sample composition is the same for the two gamma doses as well as for the fast neutrons. Analogously as for pure nickel oxide[13], a shift of the equilibrium between the various forms of surface oxygen in favour of the strongly bonded ionogenic form can be assumed to take place also in samples with extremely high nickel oxide content, where $\Delta X \approx 70\%$. Since the irradiation was conducted in air, radiative oxidation of the minority Ce^{3+} ions will play a part particularly in the other side region, and an increased concentration of detectable Ce^{4+} ions and, consequently, increased ΔX will result. The irradiation by the doses applied induces changes neither in the structure nor in the specific surface area.

TABLE II

Oxidation power of the surface of the NiO–CeO_2 systems (X), in % (m/m) O^{2-}, and the quantity normalized with respect to the surface area (X_S) in $g_{O^{2-}}\,m^{-2}$

Sample No	$X \cdot 10^{-3}$	$X_S \cdot 10^{-5}$	Sample No	$X \cdot 10^{-3}$	$X_S \cdot 10^{-5}$
1	5·2	1·2	10	51·4	1·6
2	5·6	1·2	11	46·9	2·1
3	9·9	5·0	12	45·2	2·5
4	14·6	7·9	13	44·1	2·7
5	17·6	8·2	14	36·5	2·8
6	26·4	2·4	15	28·8	3·5
7	27·4	1·5	16	38·8	2·9
8	45·5	2·4	17	29·9	2·7
9	54·8	1·5			

Kinetics of Reduction

The experimental weight losses were compared with the theoretical values for a complete reduction of nickel oxide, and this compound was found to be the only reducible component of the system at the temperatures applied. A measurable reduction of cerium dioxide to an intermediate product of the stoichiometry Ce_4O_7 was only observed at 600°C for mixed oxides containing the two constituents in a ratio of approximately 1 : 1. Sample No 1 (pure CeO_2) did not reduce in the conditions used. At lower temperatures the actual degree of nickel oxide reduction in the starting stage is markedly affected by the other constituent and increases with increasing concentration of the latter (Table III). Mixed oxides with high excess of cerium dioxide (up to 9% (m/m) NiO) were reduced at a very low rate; the reduction kinetics was not evaluated quantitatively because of the high error involved.

The kinetics of reduction of the oxides under study, over the region of degrees of reduction of $\alpha = 0{\cdot}2-1$, obeys the relation $(\alpha + 0{\cdot}3)/(1 - \alpha) = A \exp(kt)$, where α is the degree of reduction in time t, A and k are constants. The rate constants of reduction were calculated from the slope of the linear dependence of log $[(\alpha + 0{\cdot}3) : (1 - \alpha)]$ on time; generally the values increase with increasing concentration of the unreducible component up to approximately 60% (m/m) CeO_2, particularly at higher reduction temperatures (Fig. 3). The maximum reduction rate V_{max} exhibits an opposite trend (Fig. 3, curves *3*, *4*), decreasing with increasing cerium dioxide

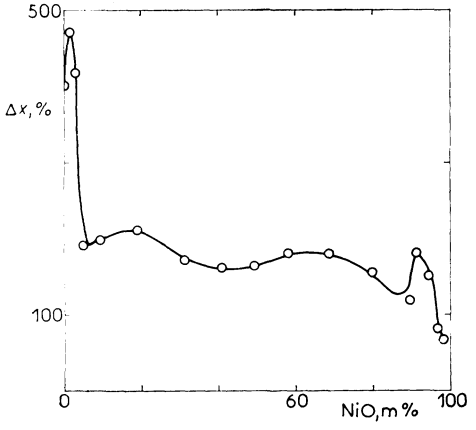

FIG, 2

Dependence of ΔX (%) on composition; gamma dose 500 kGy

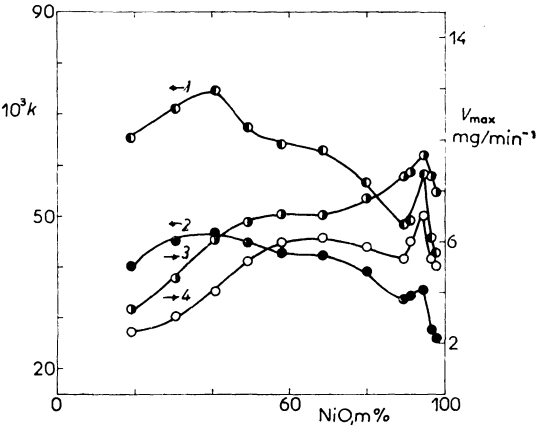

FIG. 3

Dependence of k (in relative units) *1*, *2* and V_{max} (in mg min^{-1}) *3*, *4* on composition. Temperature 350°C *2*, *4*; 410°C *1*, *3*

content except for samples with negligible amounts of this component. In contrast to homogeneous two-component systems containing a single reducible component, where both k and V_{max} decrease exponentially with increasing concentration of the unreducible component[14], the opposite trends of k and V_{max} have been observed for other heterophase-type mixed oxides[15]. Based on the microstructural analysis and morphological examination of the initial and the partly reduced samples, the mutual interaction of the two components can be assumed to be affected by steric factors which determine the positive (accelerating) as well as the retarding influence of the unreducible component on the reduction kinetics in dependence on temperature, actual degree of reduction, and system composition. In the starting stage the finely dispersed cerium dioxide blocks the active centres for the adsorption of hydrogen and the centres of nucleation of the metal product on the reaction interface; the maximum rate of reduction will decrease with increasing concentration of cerium dioxide. This is apparent particularly at higher temperatures where the reaction starts virtually simultaneously on a higher number of surface centres before the formation of the reaction zone. Cerium dioxide, however, hinders the formation of a coherent reaction zone, characterized by the maximum rate of the process. As a result of this inhibiting effect and the competitive accelerating effects, the reduction rate for samples with higher concentrations of cerium dioxide will be constant over a wide region of α values (Fig. 4, curve *3*), the sigmoid shape of the conversion curve, typical for the autocatalytic course of reduction of samples with excess nickel oxide characterized by a single sharp maximum at $\alpha \approx 0{\cdot}3$ (Fig. 4, curve *1*) will be distorted. This maximum vanishes as the cerium dioxide content is increased, and the region of constant rate grows wider. Cerium dioxide in a small fraction leads to an increase in the V_{max} value (Fig. 3). The position of the maximum in the dependence of V_{max} on composition coincides with that for the normalized amount of chemisorbed oxygen (Table II). In view of the low total cerium dioxide content, no significant influencing of the formation of the reaction interface or the nucleation

TABLE III

Degree of reduction of NiO (%) after 15 min reduction at 260 or 290°C

Sample No	260°C	290°C	Sample No	260°C	290°C
6	93·8	96·2	12	80·9	93·1
7	95·1	96·8	13	58·5	85·5
8	95·0	97·2	14	68·3	87·9
9	88·4	98·0	15	70·6	93·3
10	88·4	97·2	16	19·3	66·7
11	83·9	90·7	17	23·6	81·1

processes can be assumed in this region. The increased amount of strongly bonded ionogenic oxygen should bring about a decrease in the reduction rate owing to the retardation of the adsorption of hydrogen. Owing to the fact that in the unirradiated or untreated samples the amount of the weakly bonded neutral form of adsorbed oxygen on nickel oxide exceeds the amount of the ionogenic form by orders of magnitude[16], these samples exhibit an enhanced surface concentration of all the oxygen forms including the easily reducible neutral (physically adsorbed) form[10,13]. This is consistent with the shortening of the induction period observed for these mixed oxides.

In the following stages, on the other hand, cerium dioxide, as an "inactive" support, stabilizes the dispersity of the reducible component and of the product, inhibits the formation of a coherent layer of the metallic phase, and facilitates the transport of the reducing gas to the reaction interface. In the presence of cerium dioxide, nickel oxide thus can be completely reduced in a short time and at low temperatures (Table III).

The elementary processes associated with the irreversible adsorption of hydrogen and formation of the metal phase and the gaseous reduction product can be described as follows:

$$H_{2(g)} + 2\,O^{2-}_{lattice} \rightarrow 2\,OH^- + 2\,e^- \qquad (B)$$

$$2\,e^- + 2\,Me^{2+} \rightarrow 2\,Me^+ \qquad (C)$$

$$2\,Me^+ \rightarrow Me + Me^{2+} \qquad (D)$$

$$2\,OH^- \rightarrow (H_2O)_{ads} + O^{2-}_{lattice}\,. \qquad (E)$$

Moreover, the unmeasurable reduction of cerium dioxide,

$$Ce^{4+} + e^- \rightarrow Ce^{3+} \qquad (F)$$

can take place in the mixed system, particularly at higher temperatures. This process is associated with the liberation of oxygen atoms from the surface layers and formation of oxygen vacancies ($O^{2-}_{\square}$) according to Schottky's symbolic equation

$$H_{2(g)} \rightarrow O^{2-}_{\square} + 2\,e^- + H_2O_{(g)}\,. \qquad (G)$$

The increase in the free electron concentration can also contribute to the increase in the overall rate of reduction of the mixed oxides observed as the cerium dioxide concentration is raised. In the region of 50–70% (m/m) NiO the two counteracting processes can be assumed to be in equilibrium, so that the k and V_{max} parameters

are virtually constant, as is the apparent activation energy of reduction E_a. The fact that at lower temperatures (260–350°C) the reduction proceeds with an activation energy twice as high (in average about 120 kJ mol^{-1}) as at high temperatures (at 350 to 450°C the average value is approximately 65 kJ mol^{-1}) indicates that different active centres operate at different temperatures, the effect of the two competitive processes also varying with temperature.

The effect of irradiation on the reduction kinetic is expressed by the parameter $\Delta k\ (\%) = 100(k^* - k)/k$, where k^* and k again refer to the irradiated and non-irradiated samples, respectively. The previous irradiation of the samples has a negative effect in the region of excess nickel oxide (decrease in the reduction rate, increase in the activation energy), inverting continuously into a positive effect as the concentration of the other component is raised (Fig. 5). The region of the negative effect becomes narrower if the gamma dose is lowered, only pure nickel oxide and samples containing this oxide in an extremely high excess being reduced at a lower rate. For the irradiation by fast neutrons, the inversion of the radiation effect takes place practically at the same composition as for the irradiation by the higher gamma dose, and the shape of the dependence of Δk on composition is similar as well (Fig. 5, curves *1*, *2*).

The decrease in the reduction rate of irradiated samples containing nickel oxide in excess may be associated with the increased surface concentration of ionogenic,

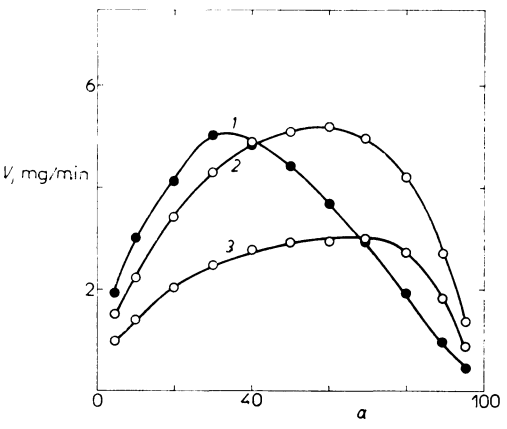

FIG. 4

Dependence of the reduction rate (in mg . min^{-1}) on the degree of reduction α at 350°C for sample No 17 *1*, 13 *2*, and 7 *3*

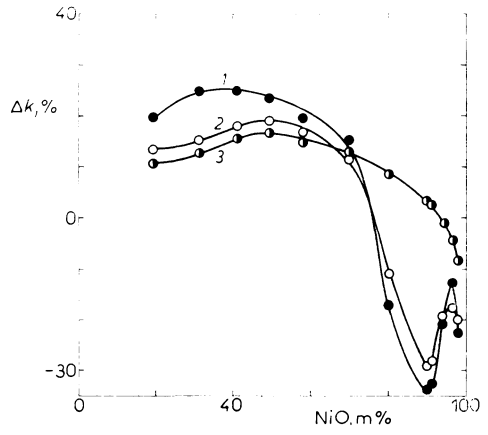

FIG. 5

Dependence of k (%) on composition for samples irradiated and reduced at 350°C. *1* fast neutrons, *2* gamma dose 500 kGy, *3* gamma dose 100 kGy

strongly bonded oxygen, leading to reduced adsorption of hydrogen owing to its donor nature. A similar effect has been observed with pure nickel oxide, whose overstoichiometry resulting from the irradiation is due principally to ionogenic oxygen[17,18]. The magnitude of the negative effect for the lower gamma dose lies beyond the overall error of determination of the rate constant. The different shapes of the dependence of Δk on composition for the two gamma doses in the negative effect region and the low absolute values of the effect for the lower of them may be due to the fact that the latter dose approaches the threshold value. Comparing the threshold gamma doses necessary for inducing measurable changes in the stoichiometry of nickel oxide[17] and in the kinetics of its reduction in various systems[19], this quantity is found highly dependent on the preparation conditions, structure and surface state[13], and, for multicomponent systems, on the composition[19]. Against the negative effect, the positive effect starts to play a part as the cerium dioxide concentration is increased. This positive effect is virtually identical for the two gamma doses applied. The pronounced temperature dependence of the positive effect indicates that the increase in the reaction rate may be due to nonequilibrium charge defects or, for fast neutrons, lattice point defects being generated by the radiation. The concentration and stabilization of the centres, which favour the reactivity of the interface and accelerate the crystallochemical conversion during the reaction, increase with increasing interaction of the two components and increasing amount of cerium dioxide with defective lattice[11]. The nonequilibrium electrons created can be trapped by surface oxygen in its neutral form, *e.g.*, by the process

$$O^0_{2(ads)} + 2\,e^- \rightarrow 2\,O^-_{ads} \qquad (H)$$

in agreement with the shift of equilibrium as discussed above. In addition, the electrons can also be captured by the biographic lattice defects, the probability of occurrence of which increases with increasing concentration of the other component.

The concentration of the ions in their higher valency, Ni^{3+} and Ce^{4+}, which are formed by ionization,

$$Ni^{2+} \rightarrow Ni^{3+} + e \qquad (I)$$

$$Ce^{3+} \rightarrow Ce^{4+} + e \qquad (J)$$

will also be higher for the irradiated samples; however, these ions are not compensated by ionogenic oxygen and so they can act as acceptor centres for a rapid adsorption of hydrogen. Their concentration increases with increasing cerium dioxide content, and so does the reduction rate. In this manner the negative radiation-induced effect inverts into a positive one.

With higher gamma doses the concentration of the radiation-induced defects can be expected to be correspondingly higher too, and so recombination processes will

increasingly play their part. Similarly as increased temperature, these recombination processes tend to lower the positive effect. This is possibly why the positive effect, at a given temperature, is little dependent on the gamma dose applied. The inversion of the effect for the reduction of samples exposed to fast neutrons can be explained similarly. However, the 20–30% decrease in the activation energy of reduction in the region of the positive effect, as compared with the unexposed samples, indicates the formation of qualitatively different centres possessing a higher reactivity, which are also sensitive to temperature changes. Here the radiation-induced lattice point defects play a major role while the charge defects resulting from secondary ionization processes play only a minor role.

Provided that the reduction proceeds at the maximum rate in the subsurface grain layer, hence, at lower degrees of conversion α, which to a first approximation is satisfied for the reduction of pure or nearly pure nickel oxide (Fig. 4), the dependence of ΔV_{max} on composition should exhibit the same trend as Δk. This assumption, based on the affecting of the purely surface process by ionizing radiation particularly in the range of the negative effect (reduced adsorption of hydrogen due to the increased concentration of ionogenic oxygen), has been proved experimentally. The magnitude of the negative effect was nearly twice as high as that expressed *via* Δk, whereas the positive effect magnitude was virtually identical. Thus, as the concentration of cerium oxide is increased, the defects generated and stabilized in the bulk start to play their positive role to a greater extent. In addition, the reaction zone region corresponding to the maximum reaction rate is displaced more inside the grain and the surface properties lose importance. In principle, V_{max} depends on the composition similarly as with unirradiated samples (Fig. 3), *i.e.*, the maximum reduction rate decreases with increasing cerium dioxide concentration. The maximum occurring in the region of high excess of nickel oxide, however, is absent for the irradiated samples, which corresponds to a lowering in the maximum reduction rate and increase in the negative radiation effect expressed by V_{max}, in agreement with the transformation of the surface oxygen into its ionogenic forms.

REFERENCES

1. Tikkanen M. N., Rosell B. O., Wiberg Ö.: Acta Chem. Scand. *17*, 513 (1963).
2. Pospíšil M., Topinka J.: This Journal *46*, 3198 (1981).
3. Vlasov V. G., Pismenko V. T., Larin A. A.: Kinet. Katal. *9*, 1094 (1968).
4. Roman A., Delmon B.: J. Catal. *30*, 333 (1973).
5. Parekh B. S., Weller S. K.: J. Catal. *47*, 100 (1977).
6. Ezhkova Z. I., Ioffe I. I., Kazanskii V. B., Krylova A. V., Lyubarski A. G., Margolic L. Y.: Kinet. Katal. *5*, 861 (1964).
7. Hattori T., Inoko J. I., Murakami Y.: J. Catal. *42*, 60 (1976).
8. Ichikava M.: J. Catal. *59*, 67 (1979).
9. Weller S. W., Volts S. E.: J. Amer. Chem. Soc. *76*, 4695 (1954).
10. Pospíšil M., Cabicar J., Rejholec V.: This Journal *35*, 1319 (1970).

11. Blumenthal R., Lee M. W.: J. Electrochem. Soc. *118*, 121 (1971).
12. Múčka V.: This Journal *42*, 391 (1977).
13. Maxim I., Braun T.: J. Phys. Chem. Solids *24*, 537 (1963).
14. Pospíšil M., Tvrzník M.: This Journal *44*, 1023 (1979).
15. Pospíšil M., Kušnierik O.: J. Therm. Anal. *25*, 499 (1982).
16. Dereň J., Stock J.: J. Catal. *18*, 249 (1970).
17. Yamashina T., Nagamatsuya T.: Bull. Chem. Soc. Jap. *38*, 507 (1965).
18. Pospíšil M., Cabicar J.: This Journal *39*, 3056 (1974).
19. Pospíšil M., Topinka J.: This Journal *42*, 391 (1977).

Translated by P. Adámek.